Genes & Nutrition

RESEARCH Open Access

Arjunolic acid inhibits Wnt3a-mediated macrophage M2 polarization to suppress osteosarcoma progression

Jun Li[1], Shuang Zhang[1], Chao Yu[1], Xia Chen[1], Weiye Zhong[1] and Yi Shen[1*]

Abstract

Background Osteosarcoma (OS) is a bone tumor characterized by a high recurrence rate and poor prognosis. Arjunolic acid (AA), the most abundant triterpene component in Cyclocarya paliurus, is reported to have anti-tumor effects. Its specific role in OS is still unknown, which we aim to investigate in our study.

Methods An OS mouse model was established to investigate the effects of AA. Subsequently, M2 macrophages and M0 macrophages pretreated with AA were co-cultured with OS cells. The impact of AA on OS cell behavior (proliferation, apoptosis, migration, and invasion) was evaluated via EdU staining, flow cytometry, and Transwell assays. Concurrently, the expression of M1- and M2-associated genes (CD86, CD163, IL-6, Arg1) was quantified to assess AA's regulatory role in macrophages within the tumor microenvironment (TME). Knockdown or overexpression of Wnt3a in AA-treated M0 macrophages to determine whether AA modulates Wnt3a-mediated M2 polarization, which was further validated in vivo.

Results In vivo, AA inhibited tumor progression in OS mice. Concurrently, AA-treated macrophages inhibited OS cell malignant behavior, and AA inhibited OS cell-mediated macrophage M2-type polarization. Mechanistically, AA inhibits the malignant behavior of OS cells and inhibits tumor progression in OS mice by suppressing Wnt3a-mediated macrophage M2 polarization. Additionally, AA-induced macrophage conversion to a pro-inflammatory phenotype in the TME of OS mice.

Conclusion Our experiment demonstrated that AA from *Cyclocarya paliurus* inhibits Wnt3a-mediated M2 macrophage polarization to suppress the progression of osteosarcoma, providing a pharmacological foundation for developing therapies against OS.

Keywords *Cyclocarya paliurus*, Arjunolic acid, Wnt3a, Macrophage M2 polarization, Osteosarcoma

Introduction

Osteosarcoma (OS) is a type of bone tumor that is most commonly seen in adolescents [1]. OS typically occurs in the long bones that bear weight, and it is characterized by a high recurrence and metastasis rate, as well as a poor prognosis [2]. Surgical treatment and chemotherapy have improved the survival rate of OS, but the overall survival rate remains low, with the possibility of recurrence [3]. Therefore, extensive research is needed to explore new treatment targets and methods for OS.

The tumor microenvironment (TME), consisting of immune cells, etc., plays a pivotal role in OS progression [4]. Tumor-associated macrophages (TAMs) are the main immune cells in TME and can be categorized into two major classes, M1 and M2 [5]. M1 macrophages possess

*Correspondence:
Yi Shen
shenyiak487@163.com
[1] Department of Orthopedics, The Second Xiangya Hospital, Central South University, No. 139 Renmin Middle Road, Furong District, Changsha, Hunan, China

anti-tumor activity, while M2 macrophages promote tumor progression [6]. Research has reported on the promotion of M1 macrophage polarization in the treatment of OS [7–9]. The level of polarization from M0 to M1 macrophages may be associated with improved prognosis in OS patients [10]. These suggest that probing the dynamic regulatory mechanisms of macrophage polarization may be therapeutically beneficial for OS.

Cyclocarya paliurus is a traditional Chinese medicine containing flavonoids, triterpenic acids, and other essential trace elements for the human body, commonly used to boost immune function or treat diseases like coronary heart disease [11]. The anticancer activity of *Cyclocarya paliurus* extract has been widely reported [12–15]. Studies have identified oleanolic acid, ursolic acid, corosolic acid, and arjunolic acid (AA), among others, as the main components of triterpenic acids in *Cyclocarya paliurus* [11]. AA is a natural small-molecule compound with antioxidant and anti-inflammatory properties [16]. It exerts antitumor effects by inducing apoptosis in Ehrlich Ascites Carcinoma cells [17]. However, despite being the predominant triterpenic component in *Cyclocarya paliurus*, the therapeutic potential of AA against OS and its underlying mechanisms remain poorly characterized.

Wnt ligands are secretory proteins that mediate intercellular interactions through paracrine or autocrine mechanisms [18, 19]. Macrophages can synthesize Wnt ligands to activate the Wnt signaling in tumor cells [18, 20]. Studies show that M2 macrophages express relatively higher levels of Wnt ligands like Wnt3 and Wnt3a compared to M1 macrophages [21]. The levels of Wnt1 and Wnt3a increase in co-cultures of M2 macrophages with thyroid cancer cells, and blocking them inhibits the malignant behavior of the co-cultured tumor cells [22]. In vitro, the Wnt3a protein promotes the polarization of M2 macrophages [23]. Conversely, a study revealed that AA suppresses Wnt3a protein overexpression [24]. This collective evidence suggests a potential mechanism through which AA mediates macrophage polarization.

Collectively, this study combines in vitro and in vivo approaches to systematically investigate the therapeutic potential of AA. We further elucidate the mechanistic basis by which AA modulates macrophage polarization and impedes OS progression, with a focus on exploring the mechanisms by which AA modulates Wnt3a-mediated macrophage M2 polarization affecting OS, thereby providing a pharmacological foundation for developing therapies against OS.

Materials and methods

Cell culture

Saos-2 cells (AW-CCH331, Abiowell) were cultured in McCoy's 5a medium (AW-MC008, Abiowell) supplemented with 10% FBS (AWC0219a, Abiowell) and 1% P/S (AWH0529a, Abiowell). U-2OS cells (AW-CCH057, Abiowell) were cultured in DMEM (AW-MC001, Abiowell) supplemented with 10% FBS and 1% P/S. THP-1 cells (AW-CCH098, Abiowell) were cultured in RPMI 1640 medium (AW-M018, Abiowell) supplemented with 10% FBS, 0.05 mM β-mercaptoethanol, and 1% P/S. The cells (Saos-2, U-2OS, THP-1) were incubated in a 95% air, 5% CO_2, 37℃ incubator. hFOB 1.19 cells (GNHu14, Stem Cell Bank, Chinese Academy of Sciences) were cultured in DMEM/F12 medium (AW-MC005, Abiowell) supplemented with 10% FBS and incubated in a 95% air, 5% CO_2, 33.5℃ incubator.

Treating THP-1 cells with phorbol 12-myristate 13-acetate (PMA, 100 ng/mL) for 48 h to obtain M0 macrophages. Inducing M0 macrophages with lipopolysaccharide (LPS, 100 ng/mL) and interferon-gamma (IFN-γ, 2.5 ng/mL) for 48 h to obtain M1 macrophages. To simulate the phenotype in the tumor microenvironment, m0 macrophages are induced with IL-4 (10 ng/mL) and IL-13(10 ng/mL) for 48 h to obtain M2 macrophages.

Cell grouping

The cells in the logarithmic growth phase were passaged and grouped for treatment according to the following experiment.

In Experiment 1, four cell types (Saos-2, U-2OS, hFOB 1.19, THP-1) were treated with different concentrations of AA (B30003, Shyuanye), including 0, 1, 5, 10, 25, 50, and 100 μg/mL for 24 h [25].

In Experiment 2, the cells were divided into the OS group, M2 + OS group, and M2 + AA + OS group. In the OS group, OS cells (Saos-2, U-2OS) were cultured at a density of 2×10^5 cells/well under normal conditions for 48 h. In the M2 + OS group, M2 macrophages were cultured normally for 24 h, then co-cultured with OS cells (Saos-2, U-2OS) at a 1:1 ratio for an additional 24 h. In the M2 + AA + OS group, M2 macrophages were treated with AA (50 μg/mL) for 24 h, followed by co-culturing with OS cells (Saos-2, U-2OS) at a 1:1 ratio for 24 h. The OS cells were collected for further analysis.

In Experiment 3, M0 macrophages were divided into the M0 group, M0 + AA, OS + M0, and AA + M0 + OS group. In the M0 groups, M0 macrophages were cultured normally. In the M0 + AA group, M0 macrophages were treated with AA (50 μg/mL). In the OS + M0 group, M0 macrophages were co-cultured with OS cells (Saos-2, U-2OS) at a 1:1 ratio. In the AA + M0 + OS group, M0 macrophages were treated with AA (50 μg/mL), followed by co-culturing with OS cells.

In Experiment 4, M0, M1, and M2 cells were each cultured normally for 24 h.

In Experiment 5, M0 macrophages were divided into M0, M0 + AA, M0 + si-NC + AA, M0 + si-Wnt3a + AA, M0 + oe-NC + AA, and M0 + oe-Wnt3a + AA groups. In the M0 + si-NC + AA, M0 + si-Wnt3a + AA, M0 + oe-NC + AA, and M0 + oe-Wnt3a + AA groups, M0 macrophages transfected with si/oe-NC and si/oe-Wnt3a plasmids respectively were treated with AA (50 μg/mL) for 24 h.

In Experiment 6, cells were divided into OS, M0 + OS, M0 + AA + OS, M0 + si-NC + AA + OS, M0 + si-Wnt3a + AA + OS, M0 + oe-NC + AA + OS, and M0 + oe-Wnt3a + AA + OS groups. In the M0 + AA + OS, M0 + si-NC + AA + OS, M0 + si-Wnt3a + AA + OS, M0 + oe-NC + AA + OS, and M0 + oe-Wnt3a + AA + OS groups, M0 macrophages transfected with si/oe-NC and si/oe-Wnt3a plasmids, respectively, were treated with AA (50 μg/mL) for 24 h, and then co-cultured with OS cells for 24 h.

Co-culture system establishment

To investigate the effects of AA on OS cells within the TME, a co-culture system was established by plating M2 macrophages in the upper chamber of Transwell plates (to simulate the TME) and seeding Saos-2 and U-2OS cells in the lower chamber. After 24 h of incubation, OS cells in the lower chamber were collected for subsequent analyses.

To investigate whether OS cells could induce M2-type polarization in macrophages, a co-culture system was established by plating M0 macrophages in the upper chamber of Transwell plates and seeding Saos-2 and U-2OS cells in the lower chamber. M0 macrophages in the upper chamber were collected after 24 h of incubation for subsequent analyses.

To investigate whether AA could modulate Wnt3a-mediated macrophage M2 polarization to affect OS cells, M0 macrophages transfected with either siRNA targeting Wnt3a (si-Wnt3a), Wnt3a-overexpressing plasmid (oe-Wnt3a), or their respective negative controls (si-NC/oe-NC), were treated with AA (50 μg/mL) for 24 h. M0 cells were then placed in the upper chamber, and Saos-2 and U-2OS cells were seeded in the lower chamber of Transwell plates to establish the co-culture system. OS cells in the lower chamber were collected after 24 h of incubation for subsequent analyses.

OS mouse model

Four-week-old male nude mice purchased from SJA Laboratory Animal Co., Ltd (Hunan, China) were adaptively fed for one week. After adaptation, 2×10^6 Saos-2 cells (100 μL per mouse) were subcutaneously injected into the armpit of the nude mice [26]. In Experiment 1, the OS mice were divided into the Model group and Model + AA group 14 days after tumor formation. In the Model + AA group, the OS mice were orally administered AA.

In Experiment 2, the nude mice were divided into Model (si-NC) + AA group, Model (si-Wnt3a) + AA group, Model (oe-NC) + AA group, and Model (oe-Wnt3a) + AA group. Mice received subcutaneous implantation of Saos-2 cells stably transfected with either si-Wnt3a, oe-Wnt3a, or si-NC/oe-NC. Mice were orally administered AA (100 mg/kg, 10 mL/kg body weight) once daily for 21 consecutive days [17]. Tumor progression was monitored twice weekly. After 35 days of tumor formation, the mice were anesthetized via intraperitoneal pentobarbital sodium (50 mg/kg), and blood samples were taken. Then the mice were euthanized, and lung tissues were taken to detect the number of metastatic nodules. The tumor tissues were photographed, measured for volume (length*width^{2}*1/2), and weighed [27].

Hematoxylin–eosin (HE) staining

To evaluate the extent of tumor lesions in OS mice and the number of metastatic nodules in lung tissue, the tumor/lung tissue slices of OS mice were first baked and then dewaxed in water. They were then stained with hematoxylin (AWI0001a, Abiowell) and eosin (AWI0029a, Abiowell), and dehydrated with a gradient of alcohol (95–100%). Finally, the slices were mounted in xylene, sealed with neutral resin, and observed under a microscope (DSZ2000X, Cnmicro).

Immunohistochemistry (IHC)

The expression of ki67 in the OS mouse tumor was first detected by adding 1% periodic acid to the tumor sections that had been baked, dewaxed, and underwent heat antigen retrieval. Then, an appropriate dilution of ki67 (27,309–1-AP, Proteintech) was added to the slices and left to incubate overnight at 4℃. The slices were washed with PBS and then incubated with HRP goat anti-rabbitIgG (AWI0629, Abiowell). After washing the slices with PBS, a DAB working solution (ZLI-9017, ZSGB-BIO) was added, followed by staining with hematoxylin. The slices were dehydrated in various grades of alcohol (60–100%), placed in xylene, and finally sealed with neutral resin for observation under a microscope.

Western blot (WB)

To detect the expression of CDK2, CDK4, and Cyclin D1 in the tumor and OS cells, and the expression of Wnt3a in macrophages, tumor tissues/cell proteins were collected with RIPA lysis buffer (AWB0136, Abiowell) and the protein concentration was measured before being subjected to electrophoresis, membrane transfer, and blocking. The nitrocellulose (NC) membranes (Invitrogen, USA) were then incubated with the primary antibody at 4℃, washed

with TBST, and incubated with the secondary antibody. Images were finally obtained using an ECL Plus detection reagent (AWB0650, Abiowell) and a gel imaging system. The internal reference is β-actin, and the antibody information is found in Table 1.

TdT-mediated dUTP nick-end labeling (TUNEL)

To detect apoptosis in murine OS tumor cells, tumor tissue slices were sequentially dewaxed, blocked, permeabilized, and biotin-blocked. Subsequently, 50 μL of TdT enzyme reaction mixture (45 μL Equilibration Buffer + 1.0 μL Biotin-11-dUTP + 4.0 μL TdT Enzyme, KGA704, KeyGen) was added to each slice sample and incubated in a light-avoiding wet box. After PBS washing, each sample was then incubated with 50 μL of Streptavidin-HRP conjugate working solution (49.5 μL 1× PBS + 0.5 μL Streptavidin-HRP) and incubated in a light-avoiding wet box. Following PBS washing, the slices were reacted with 50 μL of DAB working solution for colorization, followed by PBS washing. Subsequently, the slices were stained with hematoxylin solution, rinsed with distilled water, dipped into 1% hydrochloric acid methanol solution for 5 s, immediately rinsed with distilled water, and sequentially immersed in ethanol (70%, 85%, 95%) and xylene. After adding neutral gum and covering it with a coverslip, the section is observed under a microscope.

Cell counting kit-8 (CCK-8) assay

The cells (Saos-2, U-2OS, hFOB 1.19, THP-1) were inoculated into a 96-well plate in the past, and after the cells grew to the appropriate density, they were respectively treated according to different groups. Then, 10 μl of CCK8 medium (NU679, Abiowell, China) prepared with complete culture medium was added to each well. The plate was placed in a 37℃, 5% CO_2 incubator for 4 h. The optical density (OD) at 450 nm was analyzed using a microplate reader (MB-530, HEALES, China).

5-ethynyl-2′-deoxyuridine (EdU)

To detect the cell proliferation rate, 100 μl of 50 μM EdU medium was added to each well of the cell plate for incubation. After washing the cells with PBS and fixing them with 4% paraformaldehyde, the cells were sequentially treated with 2 mg/mL glycine and a permeabilization agent. Following another round of PBS wash, the cells were then subjected to Apollo staining and permeabilization agent decolorization. Subsequently, the cells were washed with methanol and PBS, followed by the addition of 100 μl of 1× Hoechst 33,342 reaction solution per well for incubation. Finally, the cells were washed with PBS and observed under a microscope.

Cell cycle detection

To detect the cell cycle of OS cells (Saos-2, U-2OS), the cells were suspended in PBS to separate them into individual cells before fixation. The fixed cells were centrifuged, the supernatant discarded, and then resuspended in pre-chilled PBS and centrifuged, this step was repeated twice. Next, 150 μL of propidium iodide (PI) working solution was added to the cell pellet for staining. The cells were then transferred to a flow cytometry tube for analysis.

Cell apoptosis detection

The cells, after being collected following group treatment, were suspended in 500 μL of Binding Buffer. Subsequently, 5 μL of Annexin V-APC and 5 μL of Propidium Iodide were sequentially added and mixed gently. After incubation in the dark, the cells were analyzed using a flow cytometer.

Cell migration detection

Following co-culture, the collected OS cells were resuspended in serum-free medium, and 100 μL of the cell suspension was loaded into the upper chamber of a Transwell, while 500 μL of complete medium was added to the lower chamber. The system was incubated at 37℃ for 48

Table 1 The information on antibody

Name	Dilution rate	Cat number	Source	Company	Country
CDK2	1:1000	60,312–1-Ig	Mouse	Proteintech	USA
CDK4	1:1000	11,026–1-AP	Rabbit	Proteintech	USA
Cyclin D1	1:6000	26,939–1-AP	Rabbit	Proteintech	USA
GM130	1:1000	26,744–1-AP	Rabbit	Proteintech	USA
Wnt3a	1:1000	AWA00518	Mouse	Abiowell	China
β-actin	1:5000	AWA80002	Rabbit	Abiowell	China
HRP goat anti- mouse IgG (H + L)	1:5000	SA00001-1	/	Proteintech	USA
HRP goat anti- Rabbit IgG (H + L)	1:6000	SA00001-2	/	Proteintech	USA

h. Subsequently, the upper chamber was transferred to a new well containing PBS. After the last PBS wash, cells on the upper side of the upper chamber were removed using a cotton swab. Cells adherent to the membranes were fixed with 4% paraformaldehyde, followed by staining with 0.1% crystal violet. After being washed with PBS, membranes were mounted on glass slides. Migrated OS cells were quantified by counting crystal violet-positive cells in three randomly selected microscopic fields per membrane.

Cell invasion detection

To detect the invasion of OS cells and M2 macrophages, Saos-2 and U-2OS cells were seeded in the lower chamber, while M2 macrophages were cultured in the upper chamber. After 24 h, Saos-2 and U-2OS cells were collected. Matrigel (Biocoat 356,234, Corning) diluted in 100 μL of serum-free DMEM culture medium was added to the well and incubated for 30 min, following discarding the supernatant, 100 μL of Saos-2 and U-2OS cells were added and cultured for 48 h. The cells were washed with PBS, wiped clean with cotton balls, and fixed with 4% paraformaldehyde. The membranes were then removed, stained with 0.1% crystal violet, washed with water, and observed on a glass slide.

Flow cytometry

Following PBS rinsing, cells were resuspended in 100 μL of basal culture medium. Cell suspensions were then incubated with fluorescently conjugated anti-CD86 (12–0869-42, eBioscience®), anti-CD163 (12–1639-42, eBioscience®), and isotype control antibody (Mouse IgG1κ Isotype Control PE, 12–4714-82, eBioscience®) for 30 min to account for staining. After a final PBS wash, cells were resuspended in 200 μL of staining buffer for subsequent detection.

For tumor tissue processing, minced tissues were homogenized using a mechanical tissue homogenizer (F6/10, Tissuelyser, China). The resulting murine tumor cell suspension was collected via syringe aspiration, sequentially filtered through a 100 μm cell strainer, centrifuged, and washed. Tissue homogenates were then incubated with fluorescently conjugated anti-CD86 (12–0862-82, eBioscience®), anti-CD163 (12–1631-82, eBioscience®), and isotype control antibody (Rat IgG2a kappa Isotype Control PE, 12–4321-80, eBioscience®) to account for staining. After a final PBS wash, samples were resuspended in 200 μL of staining buffer for subsequent detection.

Real-time quantitative polymerase chain reaction (RT-qPCR)

To detect the expression of IL-6, IL-1β, TNF-α, iNOS, Arg-1, IL-10, TGF-β1, MMP-9, as well as Wnt3a in macrophages and tumor tissue, total RNA was initially extracted from macrophages using Trizol, then cDNA was obtained through reverse transcription. The primers designed by Primer 5 were synthesized by Tsingke (China), which will be found in Table 2. The subsequent experiment was conducted using the UltraSYBR Mixture (CW2601, CWBio), and a fluorescence quantitative PCR instrument (SPL0960, Thermo), followed by the calculation of relative gene expression levels with the $2^{-\Delta\Delta Ct}$ method.

Table 2 Primer sequences

Gene	Sequence	Length
H-IL-6	F GCAATAACCACCCCTGACCCAA R GCTACATTTGCCGAAGAGCC	154 bp
M-IL-6	F GACTTCCATCCAGTTGCCTT ATGTGTAATTAAGCCTCCGACT	150 BP
H-IL-1β	F CCCTCTGTCATTCGCTCCC R TAAAGAGAGCACACCAGTCCA	185 bp
M-IL-1β	F TGAAATGCCACCTTTTGACAGT R TTCTCCACAGCCACAATGAGT	189 bp
H-TNF-α	F GAACCCCGAGTGACAAGCCT R TATCTCTCAGCTCCACGCCAT	120 bp
M-TNF-α	F AGCACAGAAAGCATGATCCG R CACCCCGAAGTTCAGTAGACA	162 bp
H-iNOS	F TCAGCTGTGCCTTCAACCC R CCGAGGCCAAACACAGCGTA	199 bp
M-iNOS	F GTTCTCAGCCCAACAATACAAGA R GTGGACGGGTCGATGTCAC	127 bp
H-Arg-1	F TGGACAGACTAGGAATTGGCA R CCAGTCCGTCAACATCAAAACT	102 bp
M-Arg-1	F CTCCAAGCCAAAGTCCTTAGAG R AGGAGCTGTCATTAGGGACATC	185 bp
H-IL-10	F ACCTGCCTAACATGCTTCGAGA R CTCAGCTTGGGGCATCACCT	191 bp
M-IL-10	F GTTCCCCTACTGTCATCCCC R AGGCAGACAAACAATACACCA	149 bp
H-TGF-β1	F AGCAACAATTCCTGGCGATACCTC R CAATTTCCCCTCCACGGCTCA	121 bp
M-TGF-β1	F CTCCCGTGGCTTCTAGTGC R GCCTTAGTTTGGACAGGATCTG	133 bp
H-MMP-9	F CTGAAGGCCATGCGAACCCCA R GCAAAGGCGTCGTCAATCACC	155 bp
M-MMP-9	F GCCCTGGAACTCACACGACA R GTAGCCCACGTCGTCCACC	139 bp
H-Wnt3a	F GAGCAGGACTCCCACCTAAA R GCCACCAGAGAGGAGACACT	141 bp
M-Wnt3a	F ACGTACTTCAAGGTGCCGACA R CATTTCTCCCTCCGTCGCTCA	200 bp
β-actin	F ACCCTGAAGTACCCCATCGAG R AGCACAGCCTGGATAGCAAC	224 bp

Enzyme-linked immunosorbent assay (ELISA)

According to the instructions of the IL-6 (CSB-E04639 m, Cusabio), IL-1β (CSB-E08054 m, Cusabio), TNF-α (CSB-E04741 m, Cusabio), iNOS (CSB-E08326 m, Cusabio), Arg-1 (CSB-EL002005MO, Cusabio), IL-10 (CSB-E04594 m, Cusabio), TGF-β1 (CSB-E04726 m, Cusabio), and MMP-9 (CSB-E08007 m, Cusabio) assay kits, their expressions in the serum were detected, and the Optical Density values were measured at a wavelength of 450 nm.

Statistical analysis

The data analysis software used in this experiment is GraphPad Prism 9.0, with all experimental data presented as mean ± standard deviation (SD). Student's t-test is employed for comparisons between two groups, while one-way analysis of variance (ANOVA) and two-way ANOVA are used for comparisons between multiple groups. Statistical significance is considered when $P < 0.05$.

Results

AA inhibits the progression and metastasis of cancer in OS mice

To investigate the effect of AA on OS, an OS mouse model was established. In Fig. 1A, a significant decrease in tumor volume and mass of OS mice was observed after AA intervention. HE results showed that after AA intervention, cancer cells exhibited loose arrangement, damaged texture, and an increased number of dead cells (Fig. 1B). Ki67 is a proliferation marker for OS [28]. The expression of Ki67 and cell cycle proteins (CDK2, CDK4, and Cyclin D1) in the tumor was decreased, while the apoptosis rate of tumor cells increased (Fig. 1C-F), further indicating that AA inhibits the development of OS. Additionally, H&E staining results showed a decrease in metastatic nodules in mice lung tissue after AA intervention (Fig. 1G), suggesting that AA inhibited the metastasis of OS.

AA-treated macrophages inhibit the malignant behavior of OS cells

To further confirm the effect of AA on OS, firstly, OS cells (Saos-2, U-2OS), the normal osteoblast cell line hFOB 1.19 as a control for OS cells, and THP-1 cells used to induce the formation of M2 macrophages, were all treated with different concentrations of AA. The cell viability of Saos-2 and U-2OS decreased as the concentration of AA increased, reaching a plateau at 50 μg/mL. At 100 μg/mL, the cell viability of hFOB 1.19 and THP-1 significantly decreased (Fig. 2A). Therefore, the subsequent experiments used an AA intervention concentration of 50 μg/mL, which could kill Saos-2 and U-2OS cells but not hFOB 1.19 and THP-1 cells. Co-culturing M2 macrophages with OS cells (Saos-2, U-2OS) and testing the OS cells revealed that the proliferation rate was highest in the M2 + OS group, with the shortest cell cycle arrest at the G1 phase. However, after co-culturing with AA-treated M2 macrophages, the proliferation rate of OS cells decreased, and the cell cycle arrest at the G1 phase was prolonged. (Fig. 2B-D). Further results showed that after co-culturing with AA-treated M2 macrophages, the expression of CDK2, CDK4, and Cyclin D1 in OS cells decreased, the number of cell migrations and invasion decreased, and the apoptosis rate increased (Fig. 2E-H). These results further confirm that AA-treated M2 macrophages inhibit the malignant behavior of OS cells.

AA facilitates the polarization of M0 macrophages towards the M1 phenotype and inhibits the induction of M2 polarization by OS cells

Here, we further investigated the mechanism by which AA affects macrophages in OS. Studies reported that the level of M0 to M1 macrophage polarization may be associated with the improved prognosis of OS patients [10]. CD86 is a surface marker of M1 macrophages [29], so we first examined the expression of CD86 and found that the expression of CD86 was increased in AA-treated M0 macrophages (Fig. 3A). Additionally, the expression of IL-6, IL-1β, TNF-α, and iNOS was also increased after AA treatment (Fig. 3B), suggesting that AA promotes the polarization of M0 macrophages towards the M1 phenotype.

When M0 macrophages were co-cultured with OS cells, the expression of the surface marker CD163 and Arg-1, IL-10, TGF-β1, and MMP-9 was increased (Fig. 3C-E), indicating that OS cells induce the polarization of M0 macrophages towards the M2 phenotype. Next, we investigated the effect of AA on macrophages in the tumor microenvironment (TME) and found that after AA treatment, co-culturing M0 cells with OS cells led to increased expression of CD86 and M1 macrophage-related genes (Fig. 3F-H). These results indicate that AA promotes the polarization of M0 macrophages towards the M1 phenotype and inhibits the induction of M2 polarization by OS cells.

AA inhibits Wnt3a-mediated polarization of macrophages towards the M2 phenotype

To elucidate the mechanism underlying AA-mediated inhibition of M2 macrophages polarization, we first analyzed Wnt3a expression across macrophage subtypes, revealing the highest levels in M2 and lowest in M1 macrophages (Fig. 4A). Intriguingly, AA treatment downregulated Wnt3a expression in M0 macrophages compared to untreated controls (Fig. 4B), suggesting that AA-induced Wnt3a reduction may inhibit macrophage

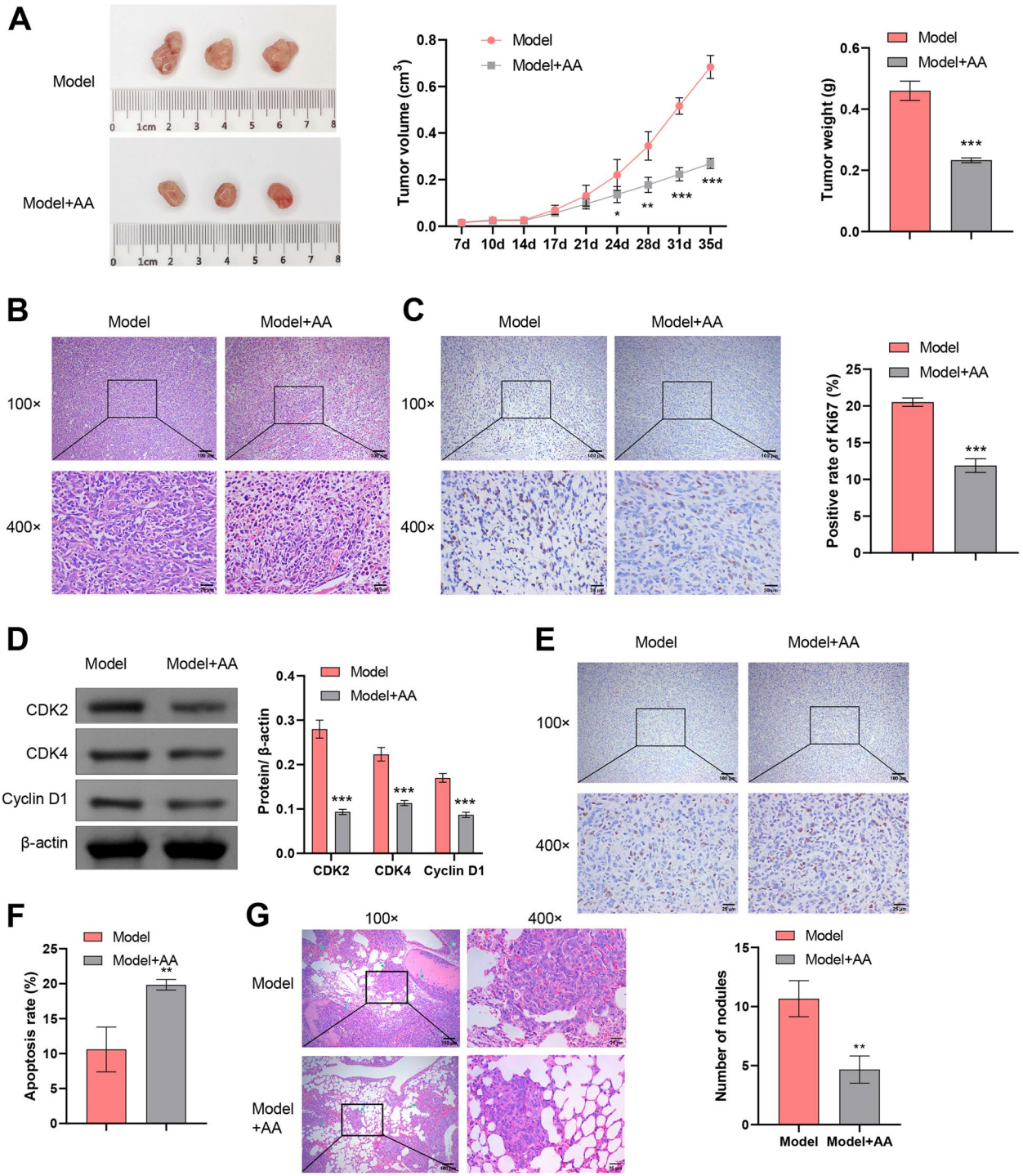

Fig. 1 AA inhibits the progression and metastasis of cancer in OS mice. **A** Tumor photographs, volume, and mass. **B** Histopathological examination of tumor changes using HE staining. **C** IHC detection of Ki67 expression in the tumor. **D** WB analysis of CDK2, CDK4, and Cyclin D1 expression in the tumor. **E**–**F** TUNEL assay for detecting tumor cell apoptosis. **G** Histopathological examination using HE staining to quantify the number of metastatic nodules in the lung tissue. *$P < 0.05$, **$P < 0.01$, ***$P < 0.001$ *vs.* Model. $n = 6$

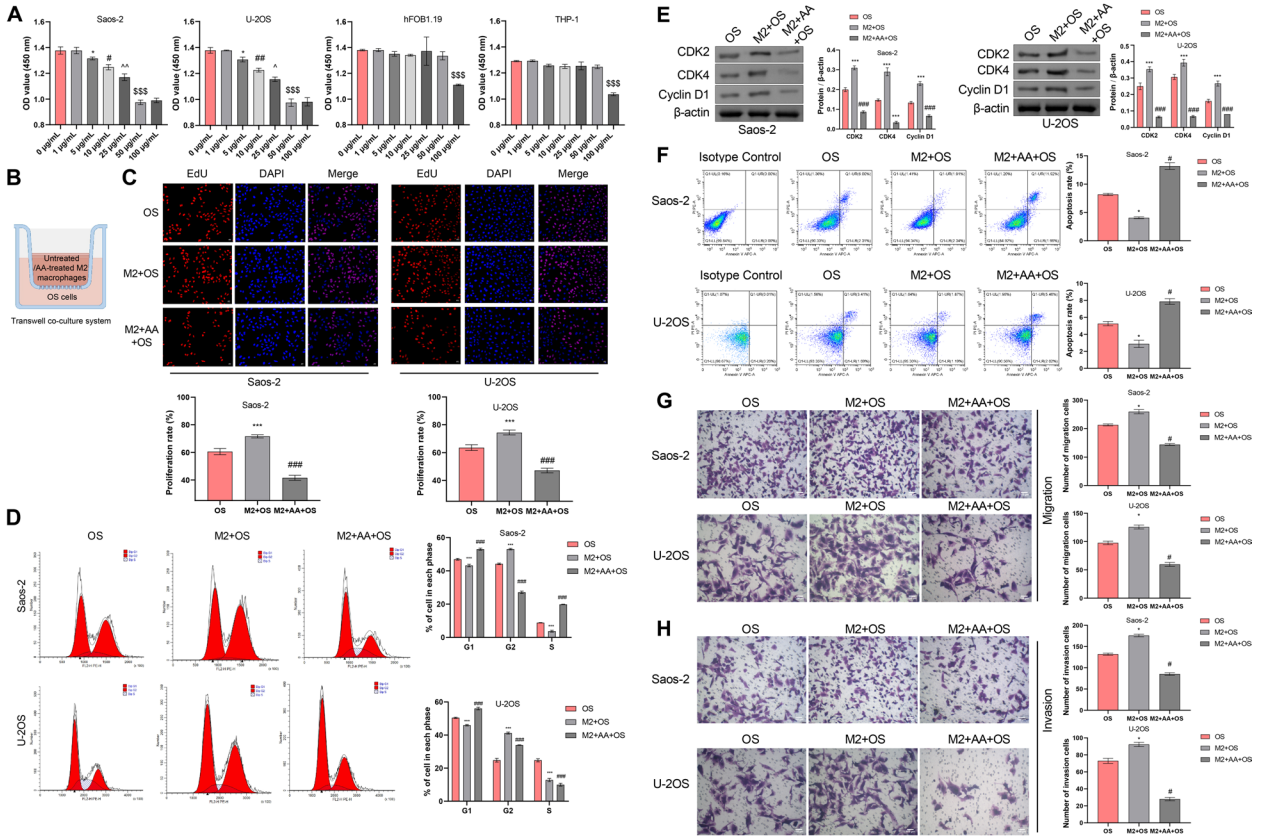

Fig. 2 AA-treated macrophages inhibit the malignant behavior of OS cells. **A** CCK-8 assay for cell viability. *$P < 0.05$ *vs.* 0 μg/mL; #$P < 0.05$ *vs.* 5 μg/mL; ^^$P < 0.01$ *vs.* 10 μg/mL; $$$$P < 0.001$ *vs.* 25 μg/mL. $n = 3$. **B** Schematic diagram of the Transwell co-culture system. **C** EdU staining to detect proliferation rate. **D** Flow cytometry analysis of cell cycle. **E** WB analysis of CDK2, CDK4, and Cyclin D1 expression. **F** Flow cytometry analysis of cell apoptosis. **G**-**H** Transwell assay for cell migration and invasion. *$P < 0.05$, ***$P < 0.001$ *vs.* OS; #$P < 0.05$, ###$P < 0.001$ *vs.* M2 + OS. $n = 3$

polarization. Subsequently, the decrease in expression with si-Wnt3a and the increase with oe-Wnt3a demonstrate the successful transfection of si/oe-Wnt3a plasmids into M0 macrophages (Fig. 4C). AA treatment suppressed M2-associated markers (CD163, Arg-1, IL-10, TGF-β1, MMP-9) levels, an effect amplified by Wnt3a knockdown and reversed by Wnt3a overexpression (Fig. 4D-E). Conversely, AA upregulated M1-associated markers (CD86, IL-6, IL-1β, TNF-α, iNOS), with Wnt3a silencing enhancing and Wnt3a overexpression attenuating these effects (Fig. 4F-G). Collectively, these findings demonstrate that AA inhibits M2 polarization by targeting Wnt3a in macrophages.

AA Suppresses OS cell malignant behavior by inhibiting Wnt3a-mediated macrophage M2 polarization

To further investigate whether AA inhibits OS progression via Wnt3a-mediated macrophage polarization, OS cells were co-cultured with macrophages transfected with Wnt3a-targeting plasmids. Figure 5A-C showed that AA treatment significantly suppressed OS cell proliferation compared to the M0 + OS group, as evidenced by reduced proliferation rates, prolonged G1 phase, and downregulated cell cycle regulators (CDK2, CDK4, cyclin D1). These anti-proliferative effects were further enhanced by Wnt3a knockdown but reversed by Wnt3a overexpression (Fig. 5A-E). Similarly, AA elevated OS cell apoptosis, a response potentiated by Wnt3a silencing and attenuated by Wnt3a overexpression (Fig. 5F). In parallel, AA inhibited OS cell migration and invasion, with Wnt3a knockdown synergistically amplifying these anti-metastatic effects, while Wnt3a overexpression restored invasive capacity (Fig. 5G-H). This indicates that the pro-inflammatory effect of TME is more significant after AA treatment.

AA induces transformation of macrophages into a pro-inflammatory phenotype in the TME of OS mice

Further in vivo experimental results show that after AA treatment, the expression of CD163 and Arg-1, IL-10, TGF-β1, and MMP-9 decreased, while the expression of CD86 and IL-6, IL-1β, TNF-α, and iNOS increased

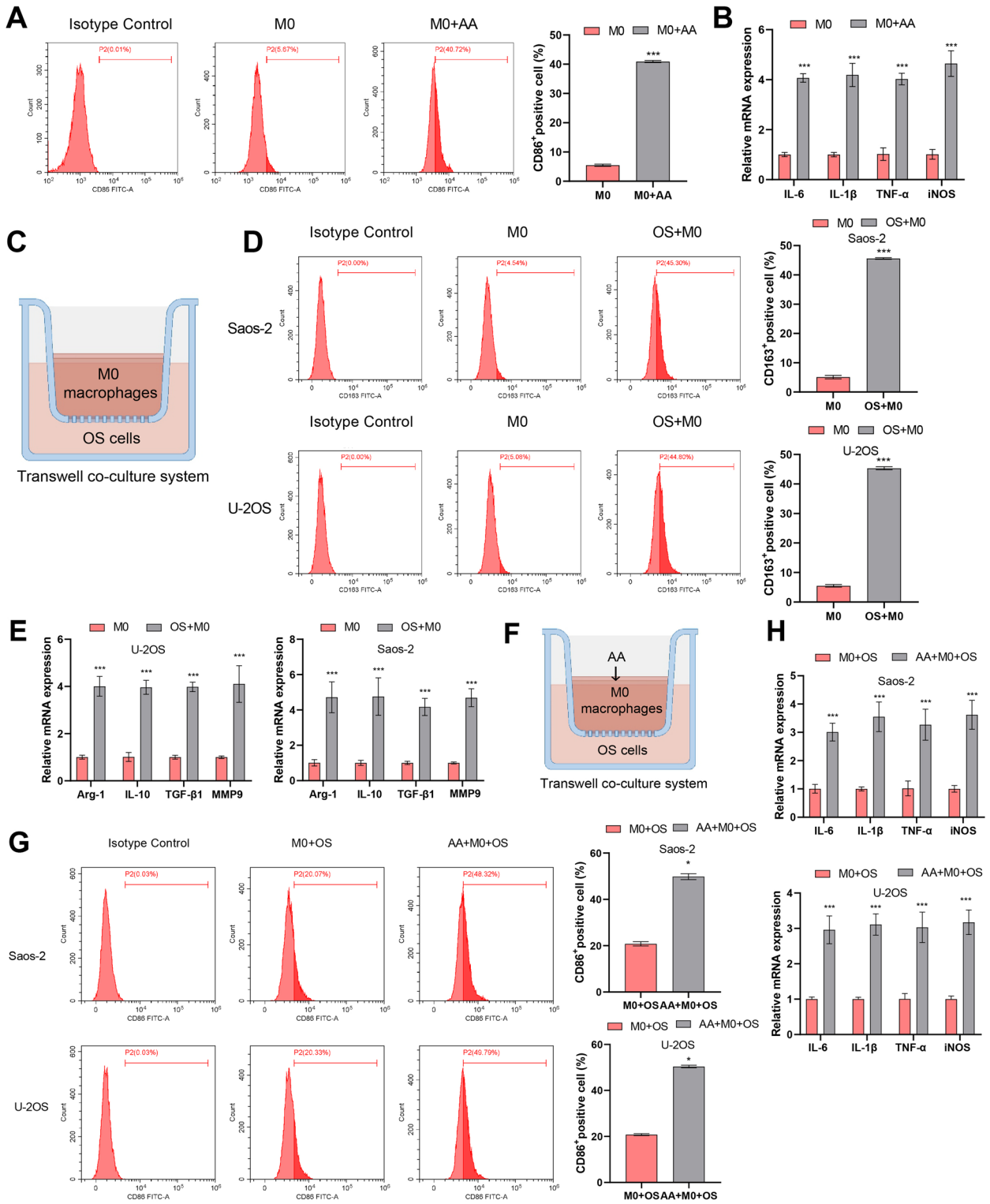

Fig. 3 AA facilitates the polarization of M0 macrophages towards the M1 phenotype and inhibits the induction of M2 polarization by OS cells. **A** C Flow cytometry analysis of CD86 expression. **B** RT-qPCR detection of IL-6, IL-1β, TNF-α, and iNOS expression. **C** Schematic diagram of the Transwell co-culture system. **D** Flow cytometry analysis of CD163 expression. **E** RT-qPCR detection of Arg-1, IL-10, TGF-β1, and MMP-9 expression. ***$P < 0.001$*vs.* M0. $n = 3$. **F** Schematic diagram of the Transwell co-culture system. **G** Flow cytometry analysis of CD86 expression. **H** RT-qPCR detection of M1 macrophage-related genes (IL-6, IL-1β, TNF-α, and iNOS) expression. *$P < 0.05$, ***$P < 0.001$ *vs.* M0 + OS. $n = 3$

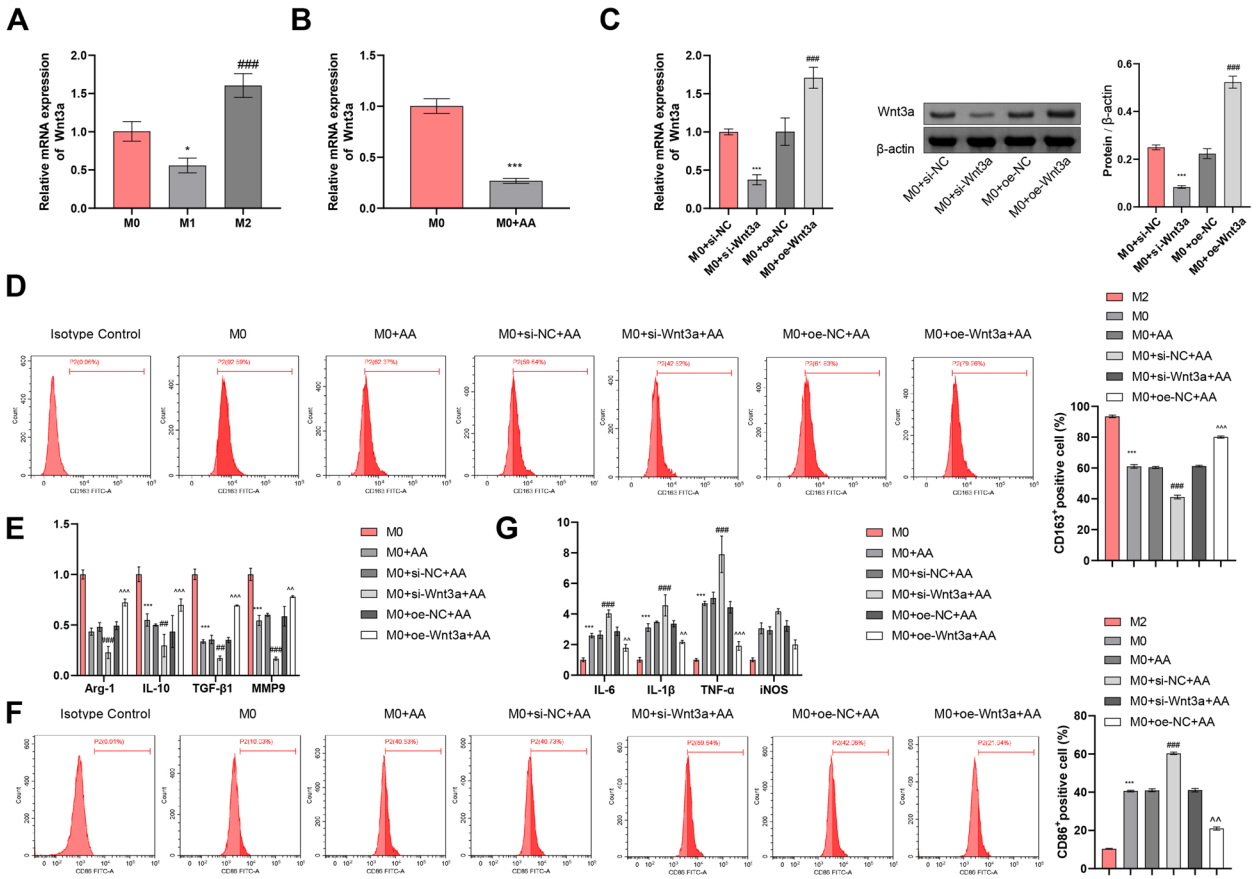

Fig. 4 AA inhibits Wnt3a-mediated polarization of macrophages towards the M2 phenotype. **A** RT-qPCR detection of Wnt3a expression. *$P < 0.05$ *vs.* M0; ###$P < 0.001$ *vs.* M1. $n = 3$. **B** RT-qPCR analysis of Wnt3a expression. ***$P < 0.001$ *vs.* M0 + AA. $n = 3$. **C** RT-qPCR analysis of Wnt3a expression. ***$P < 0.001$ *vs.* M0 + si-NC; ###$P < 0.001$ *vs.* M0 + oe-NC. $n = 3$. **D** Flow cytometry analysis of CD163 expression. **E** RT-qPCR detection of M2 macrophage-related genes (Arg-1, IL-10, TGF-β1, and MMP-9) expression. **F** Flow cytometry analysis of CD86 expression. **G** RT-qPCR detection of M1 macrophage-related genes (IL-6, IL-1β, TNF-α, and iNOS) expression. ***$P < 0.001$ *vs.* M0; ###$P < 0.001$ *vs.* M0 + si-NC + AA; ^^^$P < 0.01$, ^^^$P < 0.001$ *vs.* M0 + oe-NC + AA. $n = 3$

(Fig. 6A-F). Additionally, the expression of Wnt3a in the tumor decreased (Fig. 6G). This indicates that the pro-inflammatory effect of TME is more significant after AA treatment.

Knocking down Wnt3a further enhances the in vivo inhibitory effect of AA on OS

Through further in vivo experiments to investigate the mechanism of AA inhibition on the progression of OS, the experimental results indicate that knocking down Wnt3a leads to a decrease in mouse tumor volume and mass, reduced severity of tumor tissue pathology, and looser arrangement of cancer cells. Conversely, overexpressing Wnt3a results in an increase in tumor volume and mass, exacerbated tumor tissue pathology, and tighter arrangement of cancer cells (Fig. 7A-B). After knocking down Wnt3a, the expression of Ki67, CDK2, CDK4, and Cyclin D1 in the tumor tissue decreases, leading to an increased rate of cell apoptosis and a lower number of metastatic nodules in lung tissues. On the contrary, overexpressing Wnt3a results in the opposite effects (Fig. 7C-F). Furthermore, the expression of CD163 and Arg-1, IL-10, TGF-β1, and MMP-9 decreases with the downregulation of Wnt3a expression. Conversely, when Wnt3a expression levels increase, the expression of these markers also increases (Fig. 7G-I). In contrast, the expression of CD86 and IL-6, IL-1β, TNF-α, and iNOS increases with the decrease in Wnt3a expression, while it decreases when Wnt3a expression levels are elevated (Fig. 7J-L). Overall, the results suggest that knocking down Wnt3a could further enhance the inhibitory effect of AA on OS.

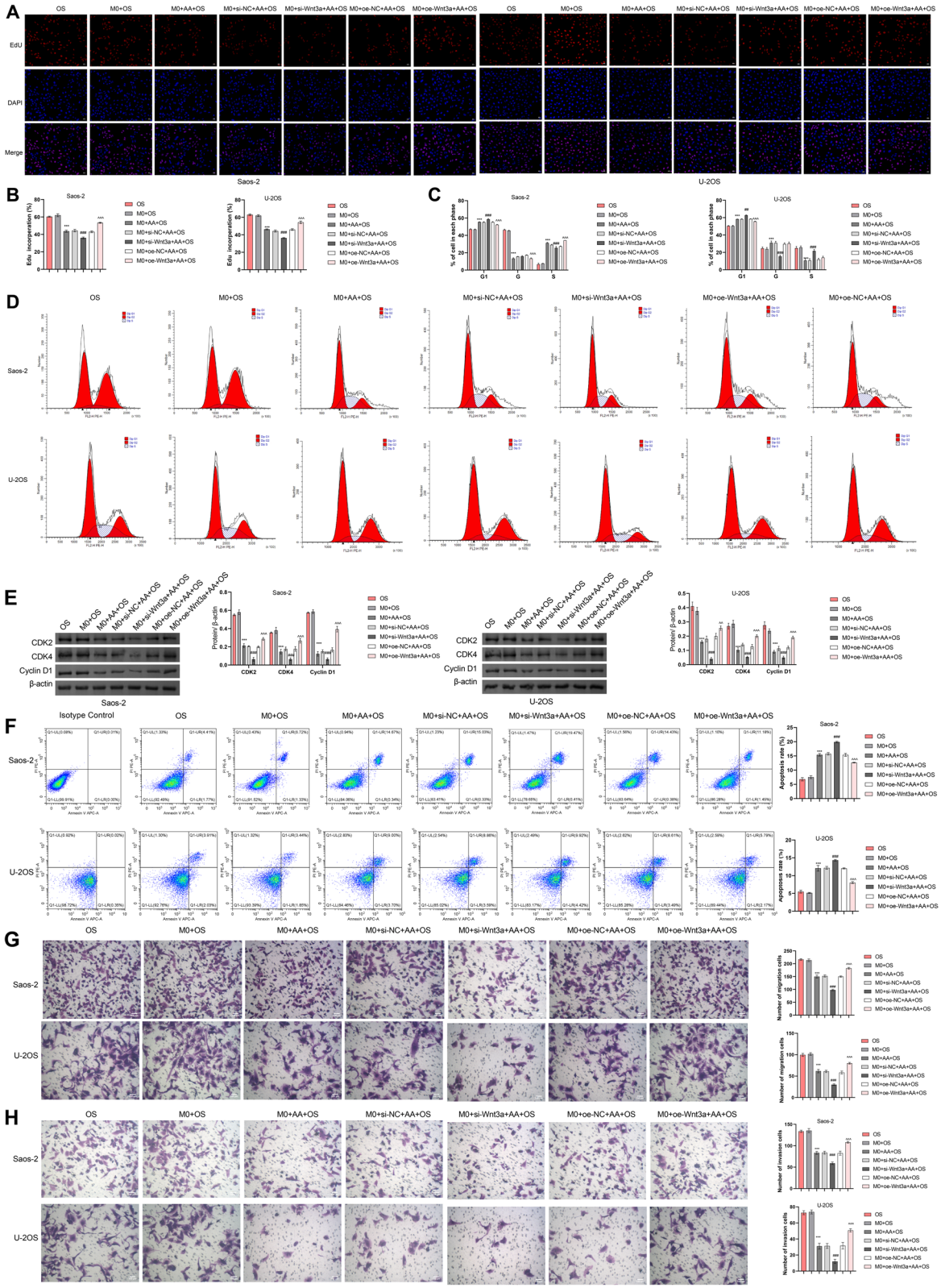

Fig. 5 AA suppresses malignant behavior of OS cells by inhibiting Wnt3a-mediated macrophage M2 polarization. **A**-**B** EdU staining to detect proliferation rate. **C**-**D** Flow cytometry analysis of cell cycle. **E** WB analysis of CDK2, CDK4, and Cyclin D1 expression. **F** Flow cytometry analysis of cell apoptosis. **G**-**H** Transwell assay for cell migration and invasion. ***$P < 0.001$ vs. M0 + OS; ###$P < 0.001$ vs. M0 + si-NC + AA + OS; ^^^$P < 0.001$ *vs.* M0 + oe-NC + AA + OS. $n = 3$

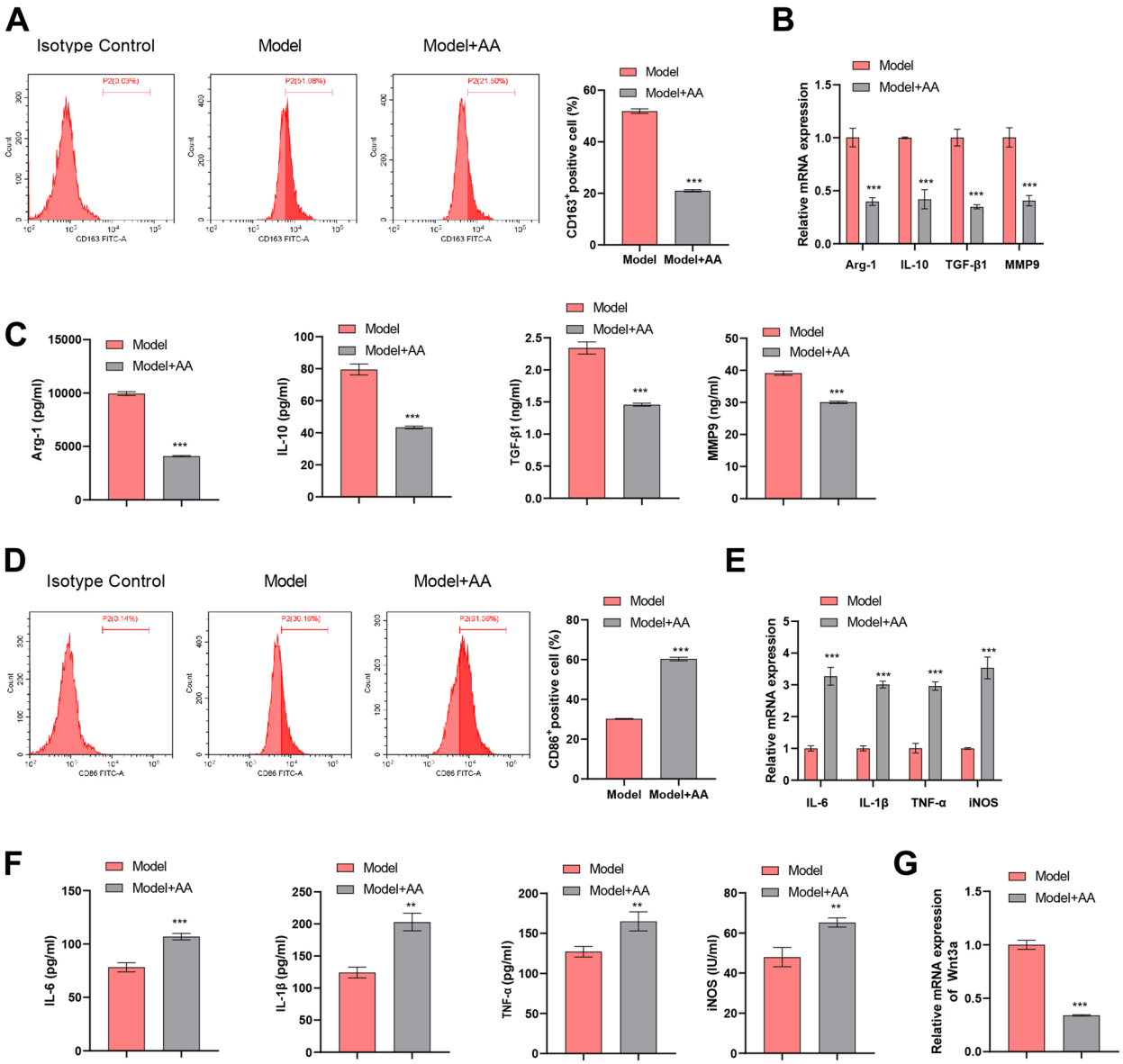

Fig. 6 AA induces transformation of macrophages into a pro-inflammatory phenotype in the TME of OS mice. **A** Flow cytometry analysis of CD163 expression in tumor tissue. **B**-**C** RT-qPCR and ELISA detection of Arg-1, IL-10, TGF-β1, and MMP-9 expression in tumor tissue and serum. **D** Flow cytometry analysis of CD86 expression in tumor tissue. **E**–**F** RT-qPCR and ELISA detection of IL-6, IL-1β, TNF-α, and iNOS expression in tumor tissue and serum. **G** RT-qPCR detection of Wnt3a expression in tumor tissue. ***$P < 0.001$ *vs.* Moedl. $n = 6$

Discussion

Originating from mesenchymal stem cells, OS is the most common primary bone tumor, with various treatment options available, but the survival rate remains relatively low [6]. AA has been shown to have anti-tumor effects, and its oral safety has been demonstrated [30]. However, its therapeutic effects in OS have not been studied. In this research, we investigated the effects of AA by constructing an in vivo mouse model of OS and found that AA inhibits the proliferation and metastasis of OS. In vitro, the viability of OS cells (Saos-2, U-2OS) significantly decreased after treatment with AA, further confirming its inhibitory effects on OS. Our study is the first to report the inhibitory effect of AA on the progression of OS. Subsequently, we further confirmed the specific mechanism of action of AA in OS through in vitro and in vivo experiments.

Macrophages are the main infiltrating immune cells in the TME and play an important role in anti-tumor immune responses, exhibiting the ability to undergo

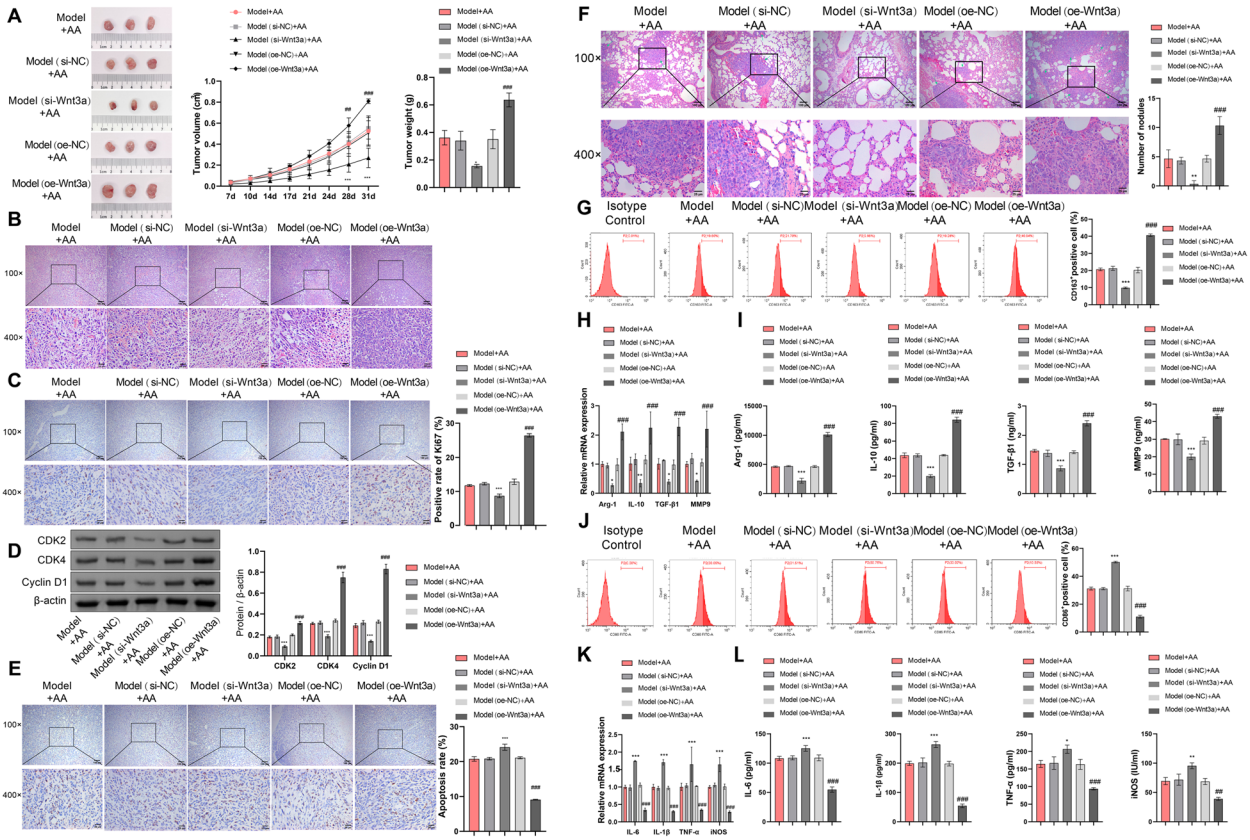

Fig. 7 Knocking down Wnt3a further enhances the in vivo inhibitory effect of AA on OS. **A** Photographs of tumor, volume, and mass. **B** HE staining to detect tumor tissue pathology. **C** IHC to detect Ki67 expression in tumors. **D** WB analysis to detect CDK2, CDK4, and Cyclin D1 expression in tumors. **E** TUNEL assay to detect cell apoptosis in tumors. **F** HE staining to detect the number of metastatic nodules in lung tissue. **G** Flow cytometry analysis of CD163 expression in tumor tissue. **H**-**I** RT-qPCR and ELISA to detect the expression of Arg-1, IL-10, TGF-β1, and MMP-9 in tumor tissue and serum. **J** Flow cytometry analysis of CD86 expression in tumor tissue. **K**-**L** RT-qPCR and ELISA to detect the expression of IL-6, IL-1β, TNF-α, and iNOS in tumor tissue and serum. ***$P < 0.001$ *vs.* Model (si-NC) + AA; ###$P < 0.001$ *vs.* Model (oe-NC) + AA. $n = 6$

phenotypic polarization [8, 31]. Research has reported that repolarization of M2-type macrophages to the M1 phenotype can reduce the expression of Programmed cell death ligand 1 (PD-L1) in OS and is an innovative cancer therapy [6]. Zhang et al. found that inhibiting M2 macrophage polarization suppresses OS metastasis [32]. In this study, we co-cultured OS cells with macrophages and found that macrophages treated with AA could inhibit the proliferation and migration of OS cells. Studies suggest that the level of polarization from M0 to M1 macrophages may be related to the improved prognosis of OS patients [10]. M1 macrophages exhibit anti-tumor activity through the expression of IL-6, IL-1β, TNF-α, and iNOS [8]. Conversely, the survival rate of OS patients may decrease when macrophages polarize towards M2-type macrophages [6]. Our results indicate that treatment with AA increased the expression of M1 macrophage-related genes (IL-6, IL-1β, TNF-α, and iNOS) in M0 macrophages, promoting the polarization of M0 macrophages towards M1 macrophages. Subsequently, we co-cultured OS cells (Saos-2, U-2OS) with M0 macrophages and found that OS cells induced polarization of M0 macrophages towards M2-type macrophages, which was inhibited by AA treatment. Additionally, in OS mice, AA treatment induced polarization of M2 macrophages in the TME towards M1 macrophages. In conclusion, AA could inhibit the polarization of macrophages towards M2 phenotype.

Wnt ligands play a role in various cancer diseases, activating the Wnt signaling pathway to promote tumor progression [33]. Yang et al.'s study indicates that Wnt ligands can stimulate macrophage M2 polarization and thus impact hepatocellular carcinoma [21]. Gao et al. reported that Zn-induced Wnt3a/β-catenin pathway can inhibit the progression of OS [34]. Our study revealed that among the three macrophage phenotypes (M0, M1, and M2), Wnt3a expression was highest in M2 macrophages. Intriguingly, AA treatment downregulated Wnt3a expression in M0

macrophages. Modulation of Wnt3a in AA-treated M0 macrophages—through either siRNA knockdown or plasmid overexpression—demonstrated that AA inhibits Wnt3a-mediated M2 polarization, as evidenced by suppressed M2 markers and elevated M1 markers. These findings were corroborated in vivo, where Wnt3a knockdown synergistically enhanced AA's anti-OS efficacy in an OS mouse model. Besides, AA induces the transformation of macrophages into a pro-inflammatory phenotype in the TME.

In conclusion, our research demonstrates that Wnt3a can mediate macrophage polarization towards the M2 phenotype and that AA could inhibit Wnt3a-mediated M2 polarization of macrophages, thereby suppressing the progression of OS. This provides a direction and insight for developing novel anti-OS drugs. The inhibitory effect of AA on Wnt3a-mediated macrophage M2 polarization contributes to a better understanding of the mechanisms underlying the development of primary bone tumors, offering new targets and strategies for clinical diagnosis and treatment. However, there are some limitations in our experiments. Although previous studies have demonstrated the safety of oral AA administration, our research did not conduct long-term observations on the efficacy of AA treatment and patient survival rates, thus, further confirmation is needed to determine its long-term efficacy and safety in clinical applications.

Acknowledgements
We would like to thank the site and instrument support provided by The First Hospital of Hunan University of Chinese Medicine.

Authors' contributions
Conceptualization: YS. Data curation and formal analysis: JL, SZ, CY, XC, and WZ. Project administration: SZ. Resources, Visualization, and Software: CY. Writing – original draft: JL. Writing – review & editing: all authors.

Funding
The study was supported by the Scientific Research Program of FuRong Laboratory(No. 2023SK2102-2) and Hunan Provincial Natural Science Foundation of China (2024 JJ7346).

Data availability
The data that support the findings of this study are available from the corresponding author, Yi Shen, upon reasonable request.

Declarations

Ethics approval and consent to participate
The Animal experiment was approved by Animal Ethics Committee of The First Hospital of Hunan University of Chinese Medicine (No. NO.20231253).

Competing interest
The authors declare no competing interests.

Received: 9 October 2024 Accepted: 9 May 2025
Published online: 21 May 2025

References

1. Ning B, Liu Y, Huang T, Wei Y. Autophagy and its role in osteosarcoma. Cancer Med. 2023;12(5):5676–87.
2. Li S, Zhang H, Liu J, Shang G. Targeted therapy for osteosarcoma: a review. J Cancer Res Clin Oncol. 2023;149(9):6785–97.
3. Shoaib Z, Fan TM, Irudayaraj JMK. Osteosarcoma mechanobiology and therapeutic targets. Br J Pharmacol. 2022;179(2):201–17.
4. Wu C, Gong S, Duan Y, Deng C, Kallendrusch S, Berninghausen L, et al. A tumor microenvironment-based prognostic index for osteosarcoma. J Biomed Sci. 2023;30(1):23.
5. Locati M, Curtale G, Mantovani A. Diversity, Mechanisms, and Significance of Macrophage Plasticity. Annu Rev Pathol. 2020;15:123–47.
6. Anand N, Peh KH, Kolesar JM. Macrophage Repolarization as a Therapeutic Strategy for Osteosarcoma. Int J Mol Sci. 2023;24(3):2858.
7. Luo G, Xu Z, Zhong H, Shao H, Liao H, Liu N, et al. Biodegradable photothermal thermosensitive hydrogels treat osteosarcoma by reprogramming macrophages. Biomater Sci. 2023;11(8):2818–27.
8. Mao X, Song F, Jin J, Zou B, Dai P, Sun M, et al. Prognostic and immunological significance of an M1 macrophage-related gene signature in osteosarcoma. Front Immunol. 2023;14:1202725.
9. Gong M, Huang Y, Feng H, Lin J, Huang A, Hu J, et al. A nanodrug combining CD47 and sonodynamic therapy efficiently inhibits osteosarcoma deterioration. J Control Release. 2023;355:68–84.
10. Liang T, Chen J, Xu G, Zhang Z, Xue J, Zeng H, et al. TYROBP, TLR4 and ITGAM regulated macrophages polarization and immune checkpoints expression in osteosarcoma. Sci Rep. 2021;11(1):19315.
11. Shen Y, Peng Y, Zhu X, Li H, Zhang L, Kong F, et al. The phytochemicals and health benefits of Cyclocarya paliurus (Batalin) Iljinskaja. Front Nutr. 2023;10:1158158.
12. Xie JH, Liu X, Shen MY, Nie SP, Zhang H, Li C, et al. Purification, physicochemical characterisation and anticancer activity of a polysaccharide from Cyclocarya paliurus leaves. Food Chem. 2013;136(3–4):1453–60.
13. Yang J, Qiu J, Hu Y, Zhang Y, Chen L, Long Q, et al. A natural small molecule induces megakaryocytic differentiation and suppresses leukemogenesis through activation of PKCδ/ERK1/2 signaling pathway in erythroleukemia cells. Biomed Pharmacother. 2019;118:109265.
14. Mo J, Tong Y, Ma J, Wang K, Feng Y, Wang L, et al. The mechanism of flavonoids from Cyclocarya paliurus on inhibiting liver cancer based on in vitro experiments and network pharmacology. Front Pharmacol. 2023;14:1049953.
15. Zhang F, Fan B, Mao L. Radiosensitizing effects of Cyclocarya paliurus polysaccharide on hypoxic A549 and H520 human non-small cell lung carcinoma cells. Int J Mol Med. 2019;44(4):1233–42.
16. Elsawy H, Almalki M, Elmenshawy O, Abdel-Moneim A. In vivo evaluation of the protective effects of arjunolic acid against lipopolysaccharide-induced septic myocardial injury. PeerJ. 2022;10:e12986.
17. Elsherbiny NM, Al-Gayyar MM. Anti-tumor activity of arjunolic acid against Ehrlich Ascites Carcinoma cells in vivo and in vitro through blocking TGF-β type 1 receptor. Biomed Pharmacother. 2016;82:28–34.
18. Pukrop T, Klemm F, Hagemann T, Gradl D, Schulz M, Siemes S, et al. Wnt 5a signaling is critical for macrophage-induced invasion of breast cancer cell lines. Proc Natl Acad Sci U S A. 2006;103(14):5454–9.
19. Liu J, Xiao Q, Xiao J, Niu C, Li Y, Zhang X, et al. Wnt/β-catenin signalling: function, biological mechanisms, and therapeutic opportunities. Signal Transduct Target Ther. 2022;7(1):3.
20. Ojalvo LS, Whittaker CA, Condeelis JS, Pollard JW. Gene expression analysis of macrophages that facilitate tumor invasion supports a role for Wnt-signaling in mediating their activity in primary mammary tumors. J Immunol. 2010;184(2):702–12.
21. Yang Y, Ye YC, Chen Y, Zhao JL, Gao CC, Han H, et al. Crosstalk between hepatic tumor cells and macrophages via Wnt/β-catenin signaling promotes M2-like macrophage polarization and reinforces tumor malignant behaviors. Cell Death Dis. 2018;9(8):793.
22. Lv J, Feng ZP, Chen FK, Liu C, Jia L, Liu PJ, et al. M2-like tumor-associated macrophages-secreted Wnt1 and Wnt3a promotes dedifferentiation and metastasis via activating β-catenin pathway in thyroid cancer. Mol Carcinog. 2021;60(1):25–37.
23. Wei Y, Yun X, Guan Y, Cao S, Li X, Wang Y, et al. Wnt3a-Modified Nanofiber Scaffolds Facilitate Tendon Healing by Driving Macrophage Polarization during Repair. ACS Appl Mater Interfaces. 2023;15(7):9010–23.

24. Aamir K, Sethi G, Afrin MR, Hossain CF, Jusuf PR, Sarker SD, Arya A. Arjunolic acid modulate pancreatic dysfunction by ameliorating pattern recognition receptor and canonical Wnt pathway activation in type 2 diabetic rats. Life Sci. 2023;327:121856.
25. Manna S, Dey A, Majumdar R, Bag BG, Ghosh C, Roy S. Self assembled arjunolic acid acts as a smart weapon against cancer through TNF- α mediated ROS generation. Heliyon. 2020;6(2):e03456.
26. Wang Z, Deng M, Chen L, Wang W, Liu G, Liu D, et al. Circular RNA Circ-03955 Promotes Epithelial-Mesenchymal Transition in Osteosarcoma by Regulating miR-3662/Metadherin Pathway. Front Oncol. 2020;10:545460.
27. Li Y, Shang C, Liu Z, Han J, Li W, Xiao P, et al. Apoptin mediates mitophagy and endogenous apoptosis by regulating the level of ROS in hepatocellular carcinoma. Cell Commun Signal. 2022;20(1):134.
28. Kim BC, Kim J, Kim K, Byun BH, Lim I, Kong CB, et al. Preliminary Radiogenomic Evidence for the Prediction of Metastasis and Chemotherapy Response in Pediatric Patients with Osteosarcoma Using (18)F-FDF PET/CT, EZRIN and KI67. Cancers (Basel). 2021;13(11):2671.
29. Zhu D, Johnson TK, Wang Y, Thomas M, Huynh K, Yang Q, et al. Macrophage M2 polarization induced by exosomes from adipose-derived stem cells contributes to the exosomal proangiogenic effect on mouse ischemic hindlimb. Stem Cell Res Ther. 2020;11(1):162.
30. Aamir K, Khan HU, Hossain CF, Afrin MR, Shaik I, Salleh N, et al. Oral toxicity of arjunolic acid on hematological, biochemical and histopathological investigations in female Sprague Dawley rats. PeerJ. 2019;7:e8045.
31. Theruvath J, Menard M, Smith BAH, Linde MH, Coles GL, Dalton GN, et al. Anti-GD2 synergizes with CD47 blockade to mediate tumor eradication. Nat Med. 2022;28(2):333–44.
32. Zhang Y, Chen Y, Chen C, Guo H, Zhou C, Wang H, Liu Z. PITX1 suppresses osteosarcoma metastasis through exosomal LINC00662-mediated M2 macrophage polarization. Clin Exp Metastasis. 2023;40(1):79–93.
33. Werner J, Boonekamp KE, Zhan T, Boutros M. The Roles of Secreted Wnt Ligands in Cancer. Int J Mol Sci. 2023;24(6):5349.
34. Gao K, Zhang Y, Niu J, Nie Z, Liu Q, Lv C. Zinc promotes cell apoptosis via activating the Wnt-3a/β-catenin signaling pathway in osteosarcoma. J Orthop Surg Res. 2020;15(1):57.

Publisher's Note